Polynomial law for controlling the generation of n-scroll chaotic attractors in an optoelectronic delayed oscillator

Bicky A. Márquez,[1, a)] José J. Suárez-Vargas,[1, b)] and Javier A. Ramírez[1]
Centro de Física, Instituto Venezolano de Investigaciones Científicas, km. 11 Carretera Panamericana, Caracas 1020-A, Venezuela

(Dated: 26 August 2014)

Controlled transitions between a hierarchy of n-scroll attractors are investigated in a nonlinear optoelectronic oscillator. Using the system's feedback strength as control parameter, it is shown experimentally the transition from Van der Pol-like attractors to 6-scroll, but in generall this scheme can produce an arbitrary number of scrolls. The complexity of every state is characterized by Lyapunov exponents and autocorrelation coefficients.

PACS numbers: 42.65.Sf, 05.45.Jn

arXiv:1408.3168v2 [nlin.CD] 23 Aug 2014

Delayed nonlinear differential equations have been implemented in electro-optical systems to generate highly complex optical chaos. These implementations in turn allowed the construction of optical communication systems with different degrees of encryption and security. However, many of those were demonstrated to be breakable by different methods of signal processing and computational analysis. Therefore, before embarking a new chaotic system in such enterprize, it would be of primary interest to characterize the dynamics using methods of phase space analysis that show hidden patterns existing in complex structures. In this report we show experiments and analysis of a time-delayed electro-optical feedback oscillator that generates an arbitrary n-scroll attractor family in a controlled fashion. This method grants a new degree of freedom when designing highly secure communication schemes, in particular it allows fine-tuning and matching the system phase-space structure with required complexity measures that maximize the security properties of a communication scheme suitably designed.

I. INTRODUCTION

Since the discovery of chaotic dynamics there has been a strong interest in finding coherent structures in systems generating very complex patterns. From the classic single[1] and 2-scroll attractors[2–4], many reports have shown systems capable of displaying hyper-chaotic n-scroll dynamics[5,6]. A number of those depend on the existence of nonlinear, non-invertible functions in their mathematical models. We highlight the work of Tang *et al.*[7] that replaces the typical nonlinear piecewise-defined function by a sine function in the Chua's circuit to generate multi-scroll attractors, and Zhong *et al.*[8] who also modified the nonlinear piecewise function in Chua's circuit to generate 10-scroll chaotic attractors. In another example Yalçin *et al.*[9] use a sine function as the nonlinear component to generate n-scroll chaotic attractors on Josephson junctions systems.

Differential equations with time delay comprise another mechanism to generate hyper-chaos[10]. In 1977 Mackey and Glass[11] proposed a first-order delayed nonlinear differential equation, which describes a physiological control system, that generates multi-scroll dynamics. Since then a significant amount of hyperchaotic systems have been defined using these equations, e.g. Wang *et al.*[12], Sprott[13] and Yalçin *et al*[14].

In this Letter, we present a general n-scroll chaotic system generated by a nonlinear delayed electro-optical feedback circuit. To build this circuit we were inspired by a modified version of the Ikeda system[15,16], and, more recently, by an electro-optic circuit able to generate a variety of dynamics, from regular to high-dimensional chaos[17].

In a previous work[18] we showed that this system has the capability to control the complexity of the dynamics by physical parameters other than the delay. In this work, we show that the law for generating n-scroll is directly related, and hence can be suitably controlled, by the number of peaks and troughs of the nonlinear, non-invertible function part of the system's transfer characteristic. Both experiments and theory supporting this discovery are detailed.

II. DELAYED NONLINEAR DIFFERENTIAL EQUATIONS

Fig. 1 we show the delayed nonlinear electro-optical feedback system[18]. It was implemented using a laser diode, a Mach-Zehnder electro-optic modulator (MZM), a photodiode, an electronic amplifier, optical fiber and a digital signal processing board (DSP) TMDSDSK6713 from Texas Instruments. The circuit is modeled by a second-order delayed nonlinear differential equation, or by a system of first-order delayed nonlinear differential equations[16]. The nonlinear transformation is im-

[a)] Email: bmarquez@ivic.gob.ve
[b)] Email: jjsuarez@ivic.gob.ve

plemented by the MZM, whose transmission function is a cosine-squared static characteristic. The modulator transforms the infrared beam, arriving from the laser through a single-mode optical fiber. The photodiode converts the output of the MZM into an electrical signal, which is time-delayed and digitally filtered with the DSP. The analog output voltage of the DSP is then amplified and connected back to the MZM radio-frequency input, $V(t)$, to form the closed loop.

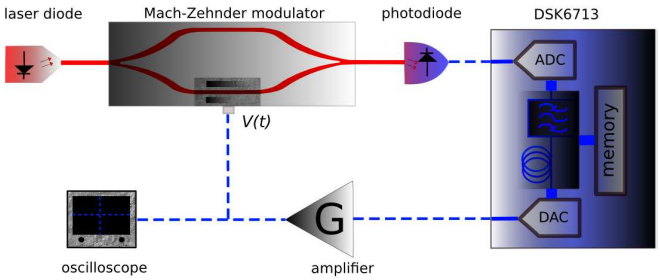

FIG. 1. Schematic diagram of the delayed feedback optical circuit that generates n-scroll hyper-chaos. It comprises a laser diode, a Mach-Zehnder modulator, a photodiode, a DSK6713 DSP board and an amplifier. The time-delay T is $10.4\mu s$, and the second-order bandpass digital filter is constructed with a low-pass filter with cutoff frequency $f_l = 1Hz$ and a high-pass filter with cutoff frequency $f_h = 10kHz$.

The system of dimensionless first-order delayed nonlinear differential equations is[15]:

$$\begin{aligned} \dot{x} &= -x - \kappa\nu - \beta\cos^2(x_\tau + \phi_0), \\ \dot{\nu} &= x; \end{aligned} \tag{1}$$

where,

$$\begin{aligned} &x(t) = \pi V(t)/2V_\pi, \quad x_\tau = x(t-\tau), \\ &\tau = 2\pi T f_h, \qquad\qquad \beta = \pi\eta G S P_{in}/2V_\pi, \\ &\kappa = f_l/f_h. \end{aligned} \tag{2}$$

The parameters are the following: dimensionless time-delay τ, feedback loop gain β, the angle describing the bias point of the modulator ϕ_0, sensitivity of the photodiode S, half-wave voltage of the MZM V_π, G is the gain of the amplifier circuit, the line attenuation factor η and f_h, f_l are cutoff frequencies of the digital bandpass filter. The experimental values are $f_l = 1Hz$ and $f_h = 10kHz$, $G = 5.5$, $V_\pi = 3.0V$, $\phi_0 = \pi/4$, $\tau = 0.65$ and the laser power is varied from $104.4\mu W$ to $1.76mW$.

III. TIME-DELAYED LIÉNARD AND VAN DER POL MODELS

To better understand the topologies of the n-scroll in the phase space we make analogies with two important mathematical systems. We begin our modeling by supposing that initially the system has no time-delay, then the planar system of Eq. (1), with $\phi_0 = \pi/4$ and $\tau = 0$, becomes

$$\ddot{x} + [1 - \beta\cos(2x)]\dot{x} + \kappa x = 0, \tag{3}$$

This equation shows that the electro-optical feedback circuit without time-delay is equivalent to a general Liénard system[19] described by the equation,

$$\ddot{x} + f(x)\dot{x} + g(x) = 0, \tag{4}$$

where $f(x) = 1 - \beta\cos(2x)$ is the even function that models the damping and $g(x) = \kappa x$ is the odd function describing the restoring force.

To find the Liénard plane associated to Eq. (1), it is necessary to derive the odd function $F(x)$ from the damping potential $f(x)$. The Liénard plane is thus defined as[20]:

$$\begin{aligned} \dot{x} &= y - F(x), \\ \dot{y} &= -g(x); \end{aligned} \tag{5}$$

where $F(x) = \int_0^x f(x')dx'$. Therefore, the Liénard plane corresponding to Eq. (3) is,

$$\begin{aligned} \dot{x} &= y - x + \beta\sin(2x)/2, \\ \dot{y} &= -\kappa x; \end{aligned} \tag{6}$$

where the odd function $F(x) = x - \beta\sin(2x)/2$. Expanding $F(x)$ in a sine Taylor series, and keeping only the first two terms, we get a Van der Pol type oscillator[20]:

$$\begin{aligned} \dot{x} &= y - (1-\beta)x + 2\beta x^3/3, \\ \dot{y} &= -\kappa x; \end{aligned} \tag{7}$$

whose corresponding potential function is given by $f(x) = 1 - \beta + 2\beta x^2$.

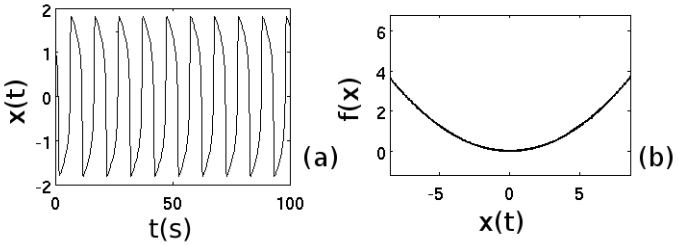

FIG. 2. (a) Numerical solution, $x(t)$, of the Van der Pol type oscillator of Eq. (7), and (b) the associated potential function $f(x)$.

The numerical solution $x(t)$ of Eq. (7) and the potential function $f(x)$ are shown in Fig. (2). The potential has a parabolic shape, which means that the dynamics is bounded on a single-well. Mono-stable potentials in systems with two degrees of freedom indicate the existence of a limit cycle, corresponding to periodic orbits.

The Liénard plane of the Van der Pol oscillator, Fig. (3), shows direction and flow velocity, and how it is affected by the shape of the potentials. The range in which

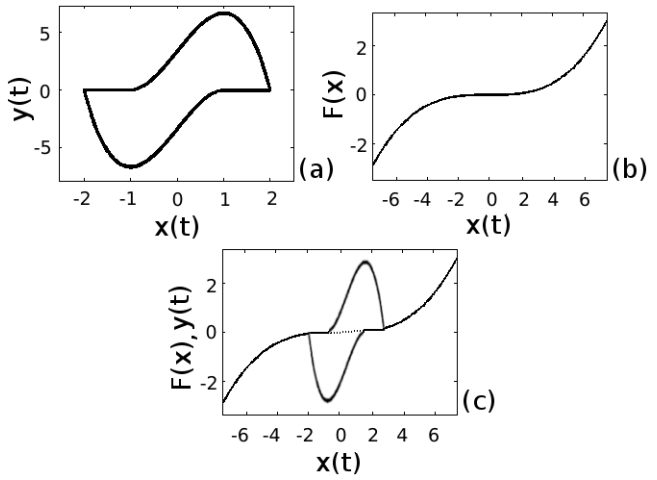

FIG. 3. (a) Phase portraits of the Van der Pol oscillator in the Liénard plane. (b) The odd function $F(x)$, and (c) overlapping the preceding figures.

the two curves are superimposed, Fig. (3-c), constitutes the epochs where the time series changes slowly, whereas the upper and lower curved protuberances of the phase plane, form fast jumps from a region to the other. The advantage of writing general systems in variables of Liénard allows us to directly observe the effect of functions associated to potentials in experimental physical systems like the optoelectronic delayed oscillator. It is well-known that a planar system, in the absence of the time-delay, cannot display chaos. By adding the time-delay, $\tau \neq 0$, there is an increase on the dimensionality of the planar system. We now write the time-delayed version of Eq. (3) that truly represents our original system model (1):

$$\ddot{x} + \dot{x} - \beta \cos(2x_\tau)\dot{x}_\tau + \kappa x = 0, \tag{8}$$

with Liénard plane:

$$\begin{aligned} \dot{x} &= y - x + \beta \sin(2x_\tau)/2, \\ \dot{y} &= -\kappa x. \end{aligned} \tag{9}$$

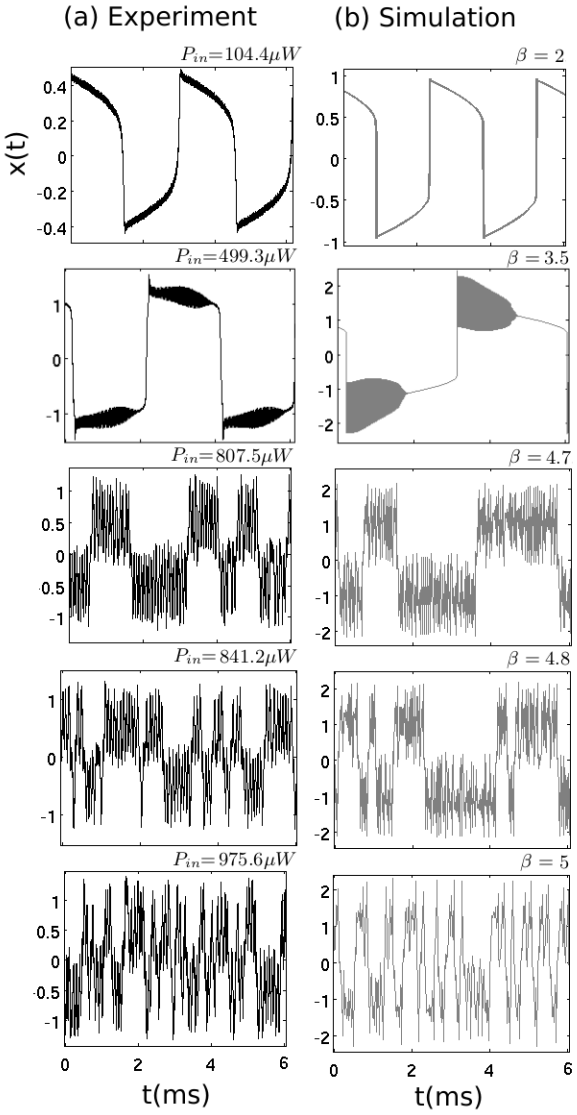

FIG. 4. Time series of the delayed electro-optical feedback system: (a) experiments and (b) simulations of Eq. (8). The laser power was changed in the values $P_{in} = \{104.4\mu W,\ 499.3\mu W,\ 807.5\mu W,\ 841.2\mu W$ and $975.6\mu W\}$. The simulation parameter was varied as $\beta = \{2,\ 3.5,\ 4.7,\ 4.8$ and $5\}$.

IV. N-SCROLL CHAOTIC ATTRACTORS FAMILY

We now use the model Eq. (8) to perform the simulations and guide the experiments. In this implementation we fixed the time-delay at $T = 10.4\mu s$, and show the route to chaos, in Fig. (4), as we vary the laser power P_{in}, in the experiments, and β in the numerical simulations. In this way we found a number of interesting bifurcations: the first bifurcation is a periodic time series occurring at $P_{in} = 104.4\mu W$, which has exactly the same shape as the Van der Pol oscillator shown in Fig. (2); in the next bifurcation, at $P_{in} = 499.3\mu W$, emerges the so-called chaotic breathers[15], they constitute the onset of chaotic oscillations *breathing* periodically; and finally we found a series of bifurcations showing chaos and n-scroll hyper-chaos.

Increasing the laser power to $P_{in} = 807.5\mu W$, Fig. (5-a), increases the number of peaks and troughs of the MZM transmission function $\cos^2$. This results in a polynomial whose degree describes the potential function of Eq. (8), $f(x) = 1 - \beta + 2\beta x^2 - 2\beta x^4/3$; therefore, the odd variable of Liénard is a polynomial of degree five in Eq. (9), $F(x) = 1 - \beta x + 2\beta x^3/3 - 2\beta x^5/15$. Because the potential function $f(x)$ is quartic, we expect to find a double-well potential that is irregularly visited by the chaotic orbits, Fig. (5-b), forming a 2-scroll chaotic at-

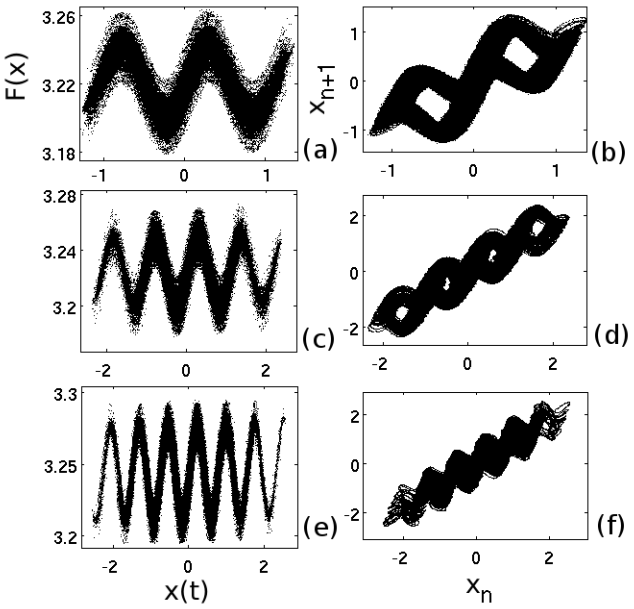

FIG. 5. (a,c,e) Transmission functions of the MZM, and (b,d,f) first return maps from the time series. In these experiments the values of laser power were $P_{in} = \{807.5\mu W$, $975.6\mu W$ and $1.76mW\}$.

tractor. When the laser power is $P_{in} = 975.6\mu W$ and $P_{in} = 1.76mW$, we obtain polynomials of degree nine and thirteen respectively, Fig. (5-c,e). In Fig. (5-d,f) we show experiments corresponding to potential functions formed by polynomials of degree eight and twelve, i.e. four-fold and six-fold potential wells. This results in 4-scroll and 6-scroll chaotic attractors.

We notice in Fig. (6) that the frequency of visits to potential wells depends on whether they are well-defined, i.e., because the polynomial is not well-formed at one of its ends, results in trajectories not visiting that region too often. Then the corresponding scroll will be less filled than in the other cases. We note also that the number of scrolls that can be obtained from this system will be greater the larger the degree of the polynomials are realized experimentally on the MZM. This poses a technological challenge for the implementation of arbitrarily large number of scrolls, and at the same time motivates the design of new systems with nonlinear characteristics that can provide this added benefit. In our particular setup using a JDSU-21014994 MZM we can only get up to a polynomial of degree thirteen, i.e., sixfold-well potential, realizing a six-scroll attractor.

V. COMPLEXITY INDICES: LYAPUNOV EXPONENT AND AUTOCORRELATION COEFFICIENT

Besides being able to discern the structure of the phase space, it is always useful to classify the attractors in terms of indices that summarize the predictability of the time

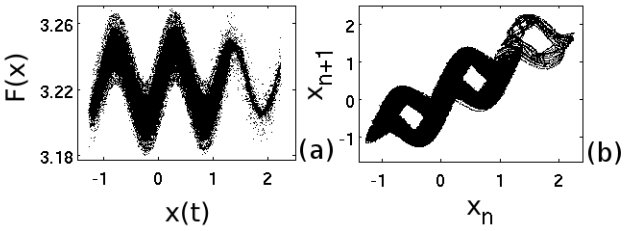

FIG. 6. (a) Transmission function of the MZM and (b) the first return map from the time-series. Laser power $P_{in} = 841.2\mu W$.

series. In Fig. (7) we show the maximum Lyapunov exponent and autocorrelation coefficient that were calculated using the software package `TISEAN`[21], for each of the n-scroll attractor generated by the electro-optical system. Both Lyapunov exponent, Fig. (7-a), and correlation coefficient, Fig. (7-b), behave monotonously, increasing the first and decreasing the latter, until the 4-scroll attractor. This means, the complexity in the system is growing proportionally with laser power. However, for 5-scroll the system unexpectedly behaves more predictable, breaking the monotony in the dependence of complexity with laser power. This behavior was observed also, for instance, in Murphy *et al.*[17], where the break of monotonous behavior was evident when the feedback intensity of their electro-optical system was increased, from $P_{in} = 841.2\mu W$.

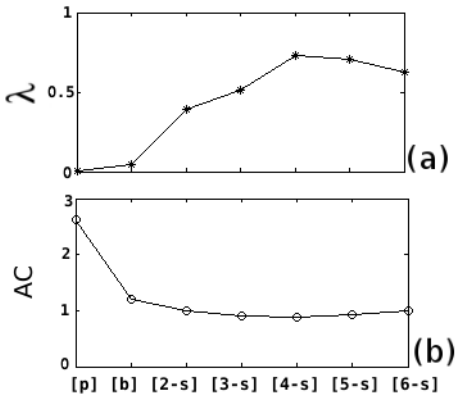

FIG. 7. Complexity indices: (a) Lyapunov exponents, λ, and (b) autocorrelation coefficients, AC, for the periodic [p], breathers [b], 2-scroll [2-s], 3-scroll [3-s], 4-scroll [4-s], 5-scroll [5-s] and 6-scroll [6-s] chaotic attractors.

VI. CONCLUSION

For a well-known optoelectronic oscillator we presented a polynomial law to predict and control the generation of n-scroll chaotic attractors, based only on the system's nonlinear static characteristic. Using the Liénard equations and phase space analysis we were able to model this electro-optical delayed feedback system, and discovered

the polynomial law that generates n-scroll chaotic attractors: the polynomial functions, $F(x)$, of degree $(N+1)$ performed by the MZM, are associated to Liénard potentials, $f(x)$, described by polynomials of degree (N), which correspond to (N/2)-scroll chaotic attractors. Importantly we associated complexity indices for each attractor structure and determined that there is a break in monotonous behavior of complexity indices Vs. laser power, as has been corroborated in other works.

ACKNOWLEDGMENTS

This work was supported under IVIC project N° 448: "Nonlinear dynamics in biological and technological systems".

[1] O. E. Rössler, Phys. Lett. **57A**, 397 (1976).
[2] E. N. Lorenz, J. Atmos. Sci. **20**, 130 (1963).
[3] T. Matsumoto, IEEE Trans. Circuits Syst. **CAS-31**, 1055 (1984).
[4] R. Brown, IEEE Trans. Circuits Syst. I, Fundam. Theory Appl.1 **40**, 878 (1993).
[5] S. Yu, J. Lu, H. Leung and G. Chen, IEEE Trans. Circuits Syst. I, Reg. Papers1 **52**, 1459 (2005).
[6] Z. Elhadj and J. C. Sprott, Int. J. Bifurcation Chaos **20**, 135 (2010).
[7] W. K. S. Tang, G. Q. Zhong, G. Chen and K. F. Man, IEEE Trans. Circuits Syst. I, Fundam. Theory Appl.1 **48**, 1369 (2001).
[8] G. Zhong, K. Man and G. Chen, Int. J. Bifurcation Chaos **12**, 2907 (2002).
[9] M. E. Yalçin Chaos, Solitons Ftactals **34**, 1659 (2006).
[10] J. C. Sprott Phys. Lett. A **228**, 271 (1997).
[11] M. C. Mackey and L. Glass, Science **197**, 287 (1977).
[12] L. Wang and X. Yang, Electron. Lett. **42**, 1439 (2006).
[13] J. C. Sprott, Phys. Lett. A **366**, 397 (2007).
[14] M. E. Yalçin and S. Özoguz, Chaos **17**, 033112 (2007).
[15] Y. Chembo Kouomou, P. Colet, L. Larger and N. Gastaud, Phys. Rev. Lett. **95**, 203903 (2005).
[16] M. Peil, M. Jacquot, Y. Chembo Kouomou, L. Larger, and T. Erneux, Phys. Rev. E **79**, 026208 (2009).
[17] T. Murphy, A. B. Cohen, B. Ravoori, K. R. B. Schmitt, A. V. Setty, F. Sorrentino, C. R. S. Williams, E. Ott, and R. Roy, Phil. Trans R. Soc. A **368**, 343 (2010).
[18] J. J. Suárez-Vargas, B. A. Márquez and J. A. González, Appl. Phys. Lett. **101**, 071115 (2012).
[19] A. Liénard, Rev. Gén. Électricité **23**, 946 (1928).
[20] S. Lynch, *Dynamical Systems with Applications using MATLAB* (Birkhauser, 2004).
[21] R. Hegger and H. Kantz, Chaos **9**, 413 (1999).